ACS Photonics

pubs.acs.org/journal/apchd5

Article

Broadband and High-Resolution Integrated Spectrometer Based on a Tunable FSR-Free Optical Filter Array

Chunlei Sun, Zequn Chen, Yuexin Yin, Yuting Ye, Ye Luo, Hui Ma, Jialing Jian, Yilin Shi, Chuyu Zhong, Daming Zhang, Hongtao Lin, and Lan Li*

Cite This: https://doi.org/10.1021/acsphotonics.2c00538

Read Online

ACCESS | Metrics & More | Article Recommendations | Supporting Information

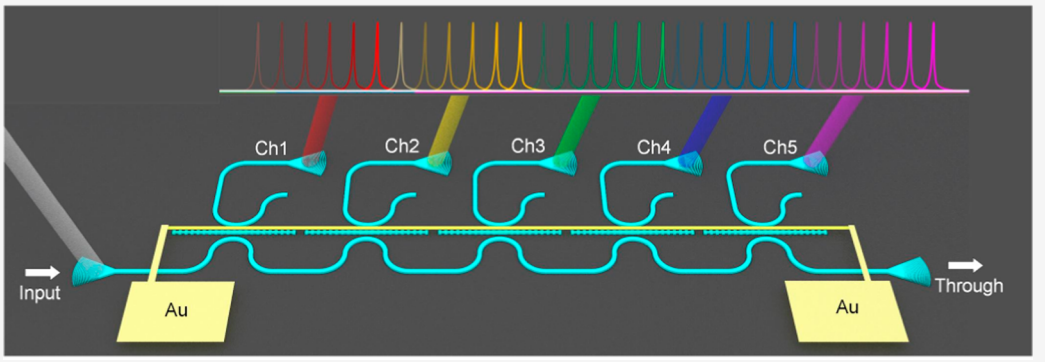

ABSTRACT: Integrated spectrometers provide the possibility of compact, low-cost portable spectroscopy sensing, which is the critical component of the lab-on-a-chip system. However, using existing on-chip designs is challenging to realize a high-resolution miniature spectrometer over a broad wavelength range. Here, we demonstrate an on-chip time-sampling narrowband filter array spectrometer that enables simultaneous acquisition of high-resolution spectra via optical Fabry−Pérot cavities and a large spectral range with tunable free spectral range free filters. Two spectrometers consisting of five and seven filter cells with a compact footprint are fabricated and experimentally characterized, demonstrating a resolution of <0.43 and <0.51 nm and a spectral range of 73.2 and 102.7 nm, respectively. Unknown broad bandwidth input signal spectra can be successfully retrieved. Integrating more filter cells with thermal isolation trenches can dramatically boost the operational spectral range. Such spectrometers may open up new pathways toward spectral analytical applications.

KEYWORDS: *integrated optics devices, optical filter, spectrometer*

INTRODUCTION

Spectrometers can provide opportunities in a wide range of fields such as biochemical sensing, materials analysis, hyperspectral imaging, and light source characterization. Developing a high-performance on-chip spectrometer is promising to activate numerous novel applications from consumer to industry technologies, including on-the-spot content analysis, instantaneous health monitoring, and even large-scale crop monitoring.[1] Integrated spectrometers based on various designs and working principles have been demonstrated since the early 1990s. Conventional integrated spectrometers utilize dispersive optics or narrowband filters to separate the spectral content of the incident signal into an array of photodetectors.[2−7] The spectral resolution of dispersive optic-based spectrometers is limited by the length of the optical path because it is inversely proportional to the optical path. Narrowband filters selecting a specific wavelength of light allow spectrometers to be more compact. The high spectral resolution is possibly achieved by introducing multiple filters with narrow channel spacing. However, the spectral bandwidth is fundamentally limited by the free spectral range (FSR).[2,6,7] For the silicon ring resonator with acceptable bend loss, the bend radius should be larger than 5 μm, indicating an FSR no larger than 19 nm around 1550 nm. Another challenge lies in inevitable fabrication imperfections for the large-scale filter array, which is crucial for small channel spacing. Fourier transform spectrometers (FTSs) can provide a higher signal-to-noise ratio compared to the conventional integrated spectrometers due to the higher received optical power or the Fellgett's advantage.[8−16] The working principle of the FTS technique is to generate a time-domain interferogram of the input signal by modulating the optical path length within an interferometer, followed by the reconstruction of the optical spectrum via a Fourier transform. However, there are several drawbacks of the FTSs, including high power consumption,

Received: April 8, 2022

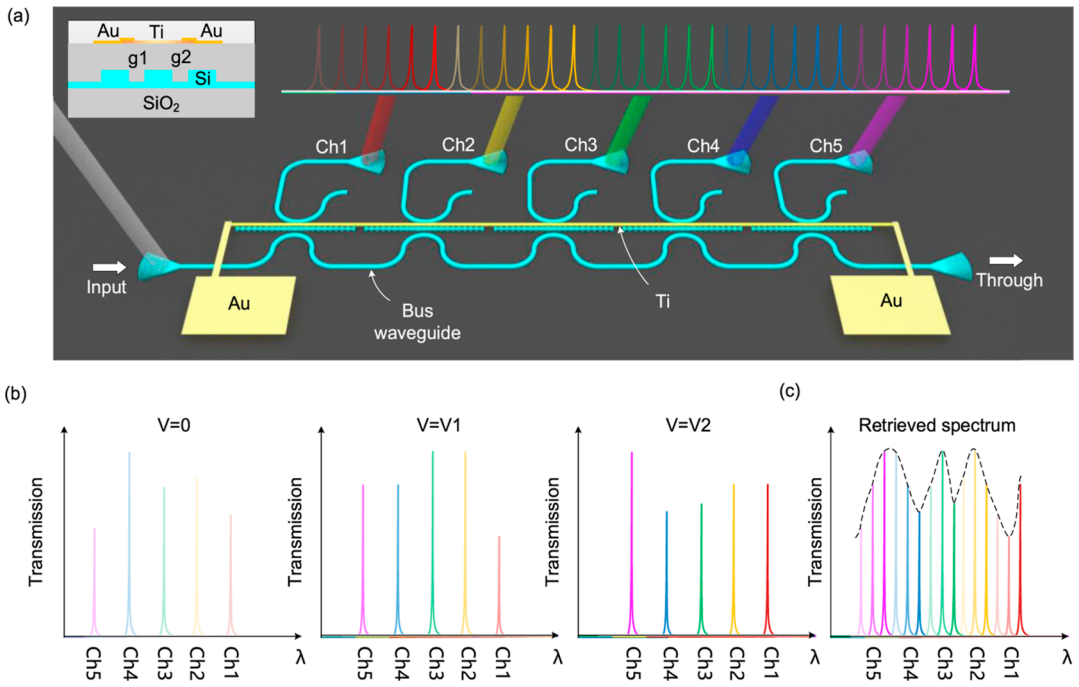

Figure 1. (a) Schematic 3D view of the TFA spectrometer based on a TFA. Inset: the waveguide cross-section of the filter. (b) Schematic of the filtered output spectra from the drop ports of the TFA spectrometer under three applied voltages (0, V1, V2). (c) Schematic retrieved spectra under different applied voltages. The original input spectrum (denoted by a dashed line) can be retrieved by combining all the retrieved spectra.

large driving voltage, long measurement time, and relatively large footprint. Over the past decade, reconstructive spectrometers, which employ scattering medium to provide a unique fingerprint (speckle) for each probe wavelength, then use computational techniques to reconstruct an incident light spectrum, have emerged.[17−21] The physical channel number and device footprint can be reduced dramatically for the sparse spectra. The critical challenges for the reconstructive spectrometer are to develop a series of speckles with an ideally orthogonal spectral response and to reduce the scattering loss within the scattering medium. In addition, the applicability to analyze complex spectra needs more computational power.

All types of integrated spectrometers possess two technical paths. One is a one-shot space sampling scheme without electrical driving/heating elements, suitable for most material platforms but sacrifices spatial occupation. To attain both broad spectral bandwidth and high spectral resolution, we must introduce a massive number of physical channels and high-performance photodetectors, which will result in a considerably large footprint, fabrication challenges, and operation complexities. Also, the other uses tunable elements for time sampling, efficiently reducing the footprint, the number of photodetectors, and enhancing the spectral resolution. Silicon is a great platform because it provides rich and efficient tuning techniques such as the thermo-optical effect, carrier dispersion, and electrostatic force. Combining space and time sampling with a few physical channels and tuning techniques is a promising way to achieve both a broad spectral bandwidth and a high spectral resolution under small space occupation.

In this paper, a compact high-resolution and broadband integrated spectrometer was proposed using a tunable filter array (TFA) to address the challenges of existing integrated spectrometers. The critical building element used to construct the micro-spectrometer is the tunable filter offering FSR-free operation to overcome the spectral range limitation. The filters are initially designed with the same resonant wavelength spacing, and the filter can route every wavelength. Leveraged by the significant thermo-optical coefficient of silicon, one can obtain an extensive tunable spectral range. Therefore, a broad spectral range can be achieved by cascading a small number of filters. Here, the filter with a double-side-coupled grating-assisted Fabry−Pérot (F−P) cavity is applied to attain FSR-free operation with a narrow bandwidth and a high rejection ratio. Furthermore, only one heater covering all the filters is used to uniformly tune the filters, simplifying the operation complexity. More importantly, the TFA spectrometer exhibits ease of scalability and flexible configuration to a broader spectral range by designing the filters covering a set of desired and even discrete wavelength bands.

DEVICE DESIGN AND OPERATION PRINCIPLE

The schematic integrated spectrometer is shown in Figure 1. The fundamental cell is the tunable filter based on a double-side-coupled grating-assisted F−P cavity, as reported in our previous work.[22] Several unit cells can be cascaded to cover a wide spectral range, where each unit is designed to cover a portion of the spectral range. The incident light propagates in the bus waveguide and then a few separated narrow spectral bands are dropped into the corresponding channels. The resonant wavelength tuning is driven by a thermo-optical heater deposited on the F−P cavity with micro-spacing. The wavelength sampling of each filter is implemented within a specific spectral range by thermal tuning. Note that the coupling strength at a longer wavelength is higher than that at a shorter wavelength. Thus, to reduce the loss caused by off-band wavelength coupling, especially in the long-wavelength range, the arrangement of the filters along the waveguide is determined by its resonant wavelengths. The filter exhibiting the longest resonant wavelength should be placed closest to

https://doi.org/10.1021/acsphotonics.2c00538
ACS Photonics XXXX, XXX, XXX−XXX

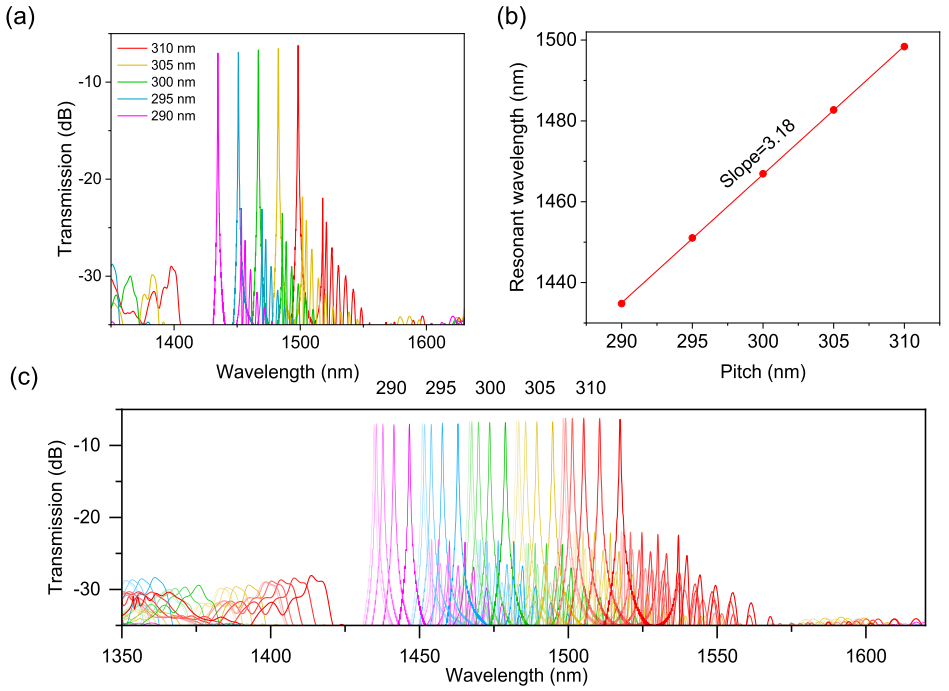

Figure 2. (a) Transmission spectra from the drop port of the filter cell with different grating pitches (290−310 nm). (b) Linear fitting between the grating pitch and the resonant wavelength. (c) Transmission spectra from the drop port of the five filter cells at different applied voltages.

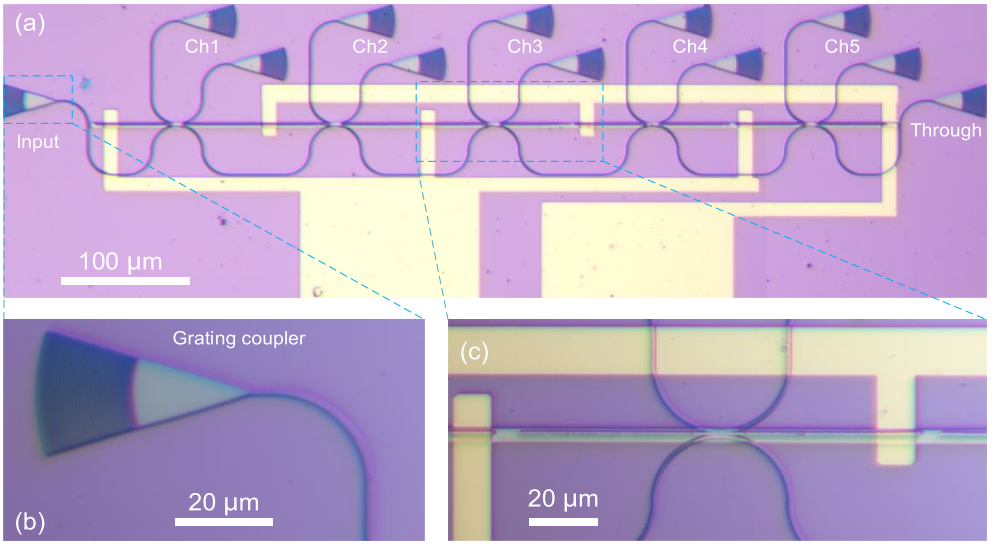

Figure 3. (a) Microscope image of the TFA spectrometer based on the five-channel filter array. Zoom-in image of the (b) grating coupler and (c) filter cell.

the input port and has high priority in extracting light from the input port. Figure 1b shows the schematic of the resonant wavelength shift under different voltages applied on the shared microheater. The wavelength shift is proportional to the heating power applied to the heater. The tunable filter in each channel can acquire the corresponding spectral information with high resolution according to the heating power and received optical power at drop ports. The full input spectrum can be retrieved by combining the spectra collected from all channels, as shown in Figure 1c. The ultimate resolution of the TFA spectrometer is decided by the thermal tuning resolution and 3 dB bandwidth of the resonant wavelength of the filter cell, which is at a sub-nanometer level. The final spectral range of the TFA spectrometer depends on the product of the tuning range of the filter cell and the filter cell number. Due to the FSR-free feature of the filter, in principle, the spectral bandwidth of the TFA spectrometer can be significantly extended by cascading numerous filter cells on a single optical link.

The position of the resonant wavelength is related to the pitch of the Bragg grating and the cavity length. The FSR-free condition is almost independent of the pitch but strongly correlates with the cavity length. Thus, we can easily choose the needed resonant wavelength and simultaneously maintain the filter's FSR-free operation capability. For ease of a representative, we cascade five filter cells into the spectrometer. Figure 2a shows the simulated spectral responses for the five filter cells with different pitches of 290, 295, 300, 305, and 310

https://doi.org/10.1021/acsphotonics.2c00538
ACS Photonics XXXX, XXX, XXX−XXX

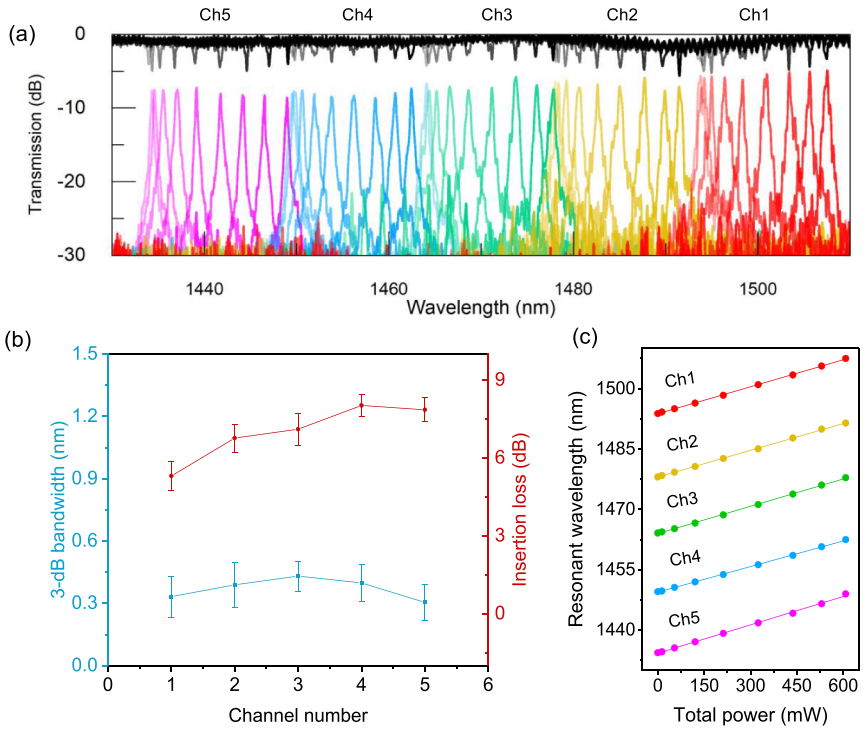

Figure 4. (a) Transmission spectra from the five channels under different applied voltages. (b) Insertion loss and 3 dB bandwidth of the filter series under various applied voltages. (c) Linear fitting of the resonant wavelength versus the heating power on the microheater.

nm. The coupling gaps g1 and g2 for the filter cells with a pitch from 290 to 310 nm are 226 to 250 nm with 6 nm intervals. The gap variation for different pitches mainly compensates for the drop efficiency due to dispersion. There are some minor transmission peaks at the red side of the main peak close to the edge of the band gap of the Bragg grating. The minor transmission peaks result from mode-mismatching between the fundamental Bloch and the waveguide mode. Thus, there are minor defects in the cavity, resulting in multiple resonance modes out of but close to the band gap, as shown in Supporting Information, Figure S1. Figure 2b exhibits an excellent linear relationship between the resonant wavelength and the pitch. The resonant wavelength red-shifts about 3.18 nm for each 1 nm increase in the pitch. The FSR-free operation is observed for all the pitches in the wavelength range from 1350 to 1630 nm. The simulated spectra of the five filter cells with the applied voltages from 0 to 5 V covers the wavelength range from 1434.8 to 1517.5 nm, as shown in Figure 2c.

DEVICE CHARACTERIZATION

Figure 3a shows the microscope image of the TFA spectrometer based on the five-channel filter array. Figure 3b,c exhibit the zoom-in images of the grating coupler and the filter cell. To reduce the total resistance of the heater, we implement a segmented microheater, as shown in Figure 3a. We can control the heater resistance without changing its total length by choosing the number of sections. Thus, we can drive the heater with a high-current/low-voltage configuration.

The transmission spectrum of the TFA spectrometer is measured with applied voltages from 0 to 8 V, as shown in Figure 4a. The insertion losses (light red dots) and 3 dB bandwidth (light blue dots) of each physical channel are shown in Figure 4b. The error bar shows the bandwidth and insertion loss variation in the same physical channel. The 3 dB bandwidth for different physical channels varies in the range of 0.30−0.43 nm. The minimum insertion loss is measured to be 5.3 dB nm, and the maximum insertion loss is 8.7 dB. The variation in the same physical channel is <1.5 dB. The off-band coupling mainly causes the insertion loss variation in different channels. The short wavelength channel usually has a slightly higher insertion loss than the long wavelength one. In addition, the coupling efficiencies of the input and output fiber-chip couplers also differ from channel to channel, as these were measured independently. The normalization of the coupling efficiency of the grating coupler increases the experimental uncertainty. However, these fluctuations do not impact the finally constructed spectra by calibration. The lowest crosstalk was measured to be −25 dB. The resolution of the TFA spectrometer is <0.43 nm, and five filter cells cover a 73.2 nm wavelength range from 1434.3 to 1507.5 nm. The resonant wavelengths of all channels are almost perfectly linear with the heating power (Figure 4c). The R-square coefficient of the linear regression fitting method, which determines the linear fitting degree, is >0.995. Note that the linear fitting degree determines the accuracy of the reconstructed spectrum. An excellent linear fitting means that the applied power can simply obtain the wavelength. The total power of the TFA spectrometer for the applied voltage of 8 V is 606 mW, and the footprint is 43 μm × 600 μm. Higher voltage than that in the simulation can be attributed to the large contact resistance and the misalignment between the grating and the microheater. The tuning range can be increased to about 30 nm by utilizing isolation trenches surrounding the filter cells.[15,23] Therefore, the spectral range of the TFA spectrometer can be extended for the same heating power and physical channel number. The normalized retrieved spectra from the five physical channels with a single-wavelength input are shown in Figure 5. We scan the applied voltage to maximize the received

https://doi.org/10.1021/acsphotonics.2c00538
ACS Photonics XXXX, XXX, XXX−XXX

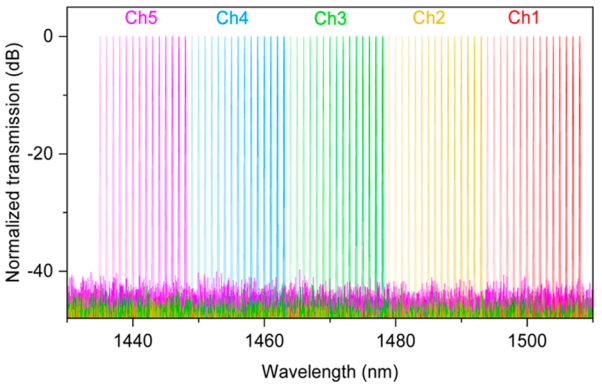

Figure 5. Normalized measured spectra from the five physical channels with a single-wavelength input.

power. A commercial spectrometer (YOKOGAWA AQ6370D) was used to attain the narrowband spectrum. We can route every wavelength in the spectral range. The wavelength increment is 1 nm from 1435 to 1508 nm for clarity.

We also experimentally characterize the TFA spectrometer based on a seven-channel filter array with the applied voltages from 0 to 8.5 V, as shown in Figure 6a. The 3 dB bandwidth varies in the range of 0.43−0.51 nm, the minimum and maximum insertion losses are 5.6 and 8.6 dB, as shown in Figure 6b. The lowest crosstalk was measured to be −20 dB. The spectral range is about 102.7 nm from 1420.9 to 1523.6 nm with a resolution of <0.51 nm. Figure 6c reveals the resonant wavelengths of all channels for the different heating power, and the R-square coefficient is >0.99. The total power for the applied voltage of 8.5 V is 873 mW, and the footprint is 43 μm × 840 μm.

As a representation of demonstration, we reconstructed the spectra by the fabricated TFA spectrometer with five channels. We first calibrated the TFA spectrometer using the TSL tunable laser with the same input power. We attained the max drop optical power at each wavelength by optimizing the applied power. Thus, the calibration (one-to-one correspondence between the input and received optical power at each wavelength) is established. The broadband spectra from the supercontinuum source were also introduced into the TFA spectrometer. We scanned the applied power and then recorded the optical power at each drop port. The input broadband spectrum is retrieved according to the relationship between the wavelength and electric power, as the colorful solid curve shows in Figure 7. The retrieved spectrum agrees well with the input one. The slight discrepancy is due to the electrical contact instability and fiber drift within measurement time. In real applications, the spectrometer can be packaged with fiber arrays as optical I/O and wire bonding as electrical I/O to avoid these instabilities. Due to the limitation of the low output power of the supercontinuum source (0 dBm at 40 MHz repetition rate) and high insertion loss of the grating coupler (>20 dB), the light with single-wavelength power lower than −33 dBm cannot be retrieved. The optical I/O configuration with higher coupling efficiency and broader bandwidth, such as edge coupler and 3D couplers, can be introduced to improve the weak light analytical capability.[24−26] In addition, the reconstruction error induced by the minor transmission peaks can be improved by the compensation algorithm (Supporting Information, Note 3).

Table 1 shows a comparison of the reported integrated spectrometers. Compared to previously reported schemes, the demonstrated TFA spectrometer can realize both high resolution and broad spectral range with a few physical channels and a compact footprint. The reconstructive

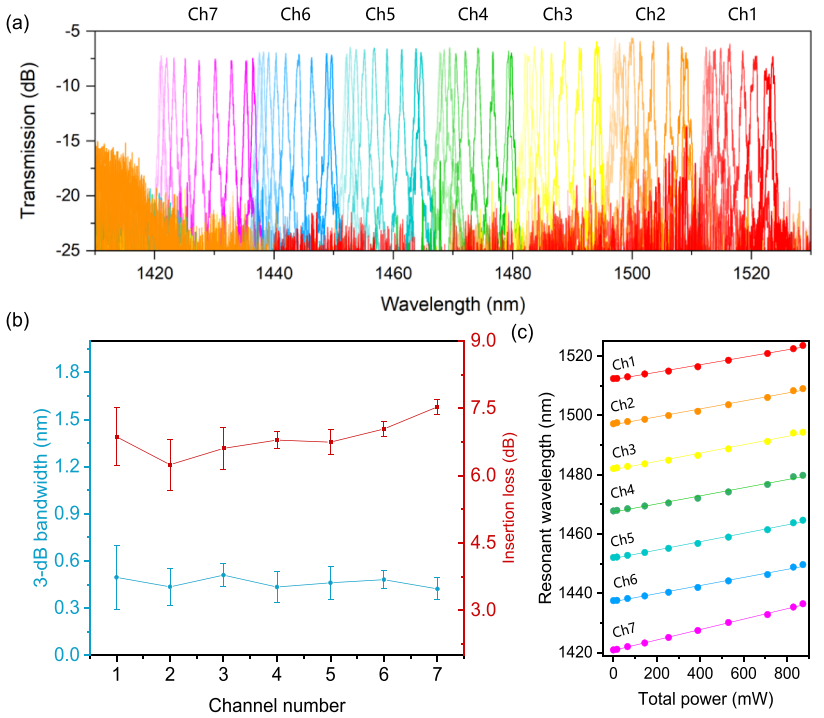

Figure 6. (a) Transmission spectra from the seven channels under different applied voltages. (b) Insertion loss and 3 dB bandwidth of the filter series for various applied voltages. (c) Linear fitting of the resonant wavelength versus the heating power on the microheater.

https://doi.org/10.1021/acsphotonics.2c00538
ACS Photonics XXXX, XXX, XXX−XXX

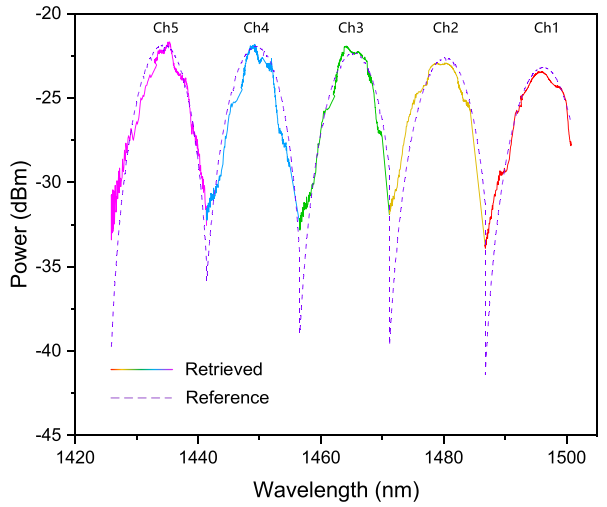

Figure 7. Retrieved spectra from the five channels (solid line) by the TFA together with a reference measurement (dashed line) by the commercial spectrometer.

spectrometer is also a powerful tool to analyze spectra with high resolution and broad spectral range. However, the reconstructive error of reconstructive spectrometers is a strong correlation with the complexity of the spectrum.[18] Generally, the more complex the spectrum, the higher the error. The reconstructive spectrometers are desired to recover particular and simple spectra by the compressive sensing method. A complex spectrum (e.g., the dense spectrum contains a lot of narrow spectral lines or contains both sharp and smooth features) requires a complex reconstruction model with many parameters and huge computation power.[16,21] Our proposed TFA spectrometer only needs a simple spectral construction process for general spectra. Meanwhile, the bandwidth can be easily broadened by integrating more filter cells.

DISCUSSION

The designed TFA spectrometer using a tunable FSR-free filter array realizes high-resolution and large-range spectral analysis. The final resolution is the minimum of the linewidth of the resonance peak and the minimum tuning wavelength interval. The smaller the minimum tuning wavelength interval is, the higher the resolution is. However, it results in severe crosstalk and a smaller dynamic range (Supporting Information, Note 2). For the five-channel TFA spectrometer, the measured 10−90% increase and 90−10% fall times are 5.9 and 8.0 μs (Supporting Information, Figure S3). The one-time scan duration is 0.3 s, and the corresponding energy consumption to implement a full-range scan is about 181.8 mJ (Supporting Information, Note 4).

CONCLUSIONS

In summary, we proposed and demonstrated a compact high-resolution and large spectral range integrated spectrometer by using a tunable FSR-free filter array. Each filter unit is designed to cover a portion of the input spectrum, and the time-sampling technique by tunable elements dramatically decreases the number of physical channels. Due to the high-quality factor of the F−P cavity, the resolution of the TFA spectrometer is dramatically boosted beyond the conventional spatial-sampling narrow-filter-based spectrometer by finely tuning the resonance wavelength. The FSR-free operation of the filter overcomes the spectral range limitation. As a demonstration, five-channel and seven-channel spectrometers are fabricated and experimentally characterized, demonstrating resolution of <0.43 and <0.51 nm and a spectral range of 73.2−102.7 nm. The power consumption due to thermal tuning can be drastically reduced by introducing isolation trenches. The TFA spectrometer has good scalability, can be extended to a broader spectral range, and can be flexibly configured by designing a set of filters covering required or even discrete bands.

Table 1. Comparison of Reported Integrated Spectrometers

schemes	resolution $\Delta\lambda$/nm	range/central wavelength/nm	spectral channels	physical channels	size/mm^2	power/mW	applicability of spectral analysis
digital planar holograms[4]	0.15	148/600	987	987	2	0	general
arrayed waveguide gratings + microring[5]	0.1	25.4/1555	254	9	9	363	general
microdonut array[6]	0.6	50/1580	84	84	1	0	general
diffraction grating + microring[7]	0.1	10/1488	100	10	2		general
coiled spirals based Fourier transform[10]	0.04	0.75/1550	18	32	12	0	general
spatial heterodyne Fourier transform[11]	0.085	0.6/1568	7	16	4.5	0	general
stationary-wave integrated Fourier transform[12]	5.5	500/1550	91	1	10		general
Fourier transform[13]	3.1	56.2/1550	18	1	1	2500	general
multimode Fourier transform[14]	0.88	60/1550	68	1		5200	general
microring assisted Fourier transform[15]	0.47	90/1571	191	1		1835	general
digital Fourier transform[16]	0.2	4.8/1560	24	1		99	particular type
random structure[17]	0.75	25/1512	33	25	0.005	0	particular type
multimode spiral waveguide[18]	0.01	2/1520	200	40	0.25	0	particular type
linear coherent network[19]	0.02	12/776	600	64	0.01144	0	particular type
tailored disorder modes[20]	0.25	30/1555	120	8	0.00039	0	particular type
stratified waveguide filters[21]	0.45	180/1560	400	32	0.0126	0	particular type
our work	0.43	73.2/1472	170	5	0.0258	606	general
our work	0.51	102.7/1472	201	7	0.03612	873	general

https://doi.org/10.1021/acsphotonics.2c00538
ACS Photonics XXXX, XXX, XXX−XXX

MATERIALS AND METHODS

Numerical Simulation Method. The transmission response of the tunable filter is calculated by using the 3D finite difference time domain numerical method. Scattering bound condition is taken into account and a perfectly matched layer is used to surround the simulation domain. The temperature field distributions of the filter at different bias voltages using the finite-element solver realize external wavelength tuning.

Device Fabrication. The TFA spectrometer was fabricated on a 220 nm silicon-on-insulator platform with the processes of patterning structures by electron beam lithography (Raith Voyager) and subsequent dry etching through inductively coupled plasma (Samco). First, a shallow etching with a depth of 150 nm was executed to form the waveguides and grating couplers. Then, a 1 μm-thick silica thin film was deposited to cover the entire device by utilizing the plasma-enhanced chemical vapor deposition process. Finally, the contact pads and thermo-optical microheaters were defined by an ultraviolet lithography process, followed by the deposition of the metal titanium and gold with different thickness combinations utilizing e-beam evaporation (10 nm Ti/100 nm Au for contact pads and 100 nm Ti/10 nm Au for microheaters). All the filters were tuned at the same time by the heater. The width of the microheater is 2.75 μm.

Experimental Method. The spectral responses of the TFA spectrometer were characterized by a broadband tunable laser system (Santec full-band TSL, 1260−1630 nm), launching light into the input port and monitoring the transmissions at the drop ports of the filter cells. The measured spectral responses were normalized concerning the transmission of the reference grating couplers on the same chip. The resolution is 10 pm in the measurements. A broadband spectrum from a supercontinuum source (YSL SC-Pro) with an acousto-optic tunable filter (YSL AOTF) as an input broadband signal was used to test the performance of the TFA spectrometer. The AOTF had a 3 dB bandwidth of 10 nm, and the central wavelength was set at 1434, 1449, 1465, 1480, and 1496 nm, respectively. The commercial spectrometer (YOKOGAWA AQ6370D) recorded the broadband spectra as the reference.

ASSOCIATED CONTENT

Supporting Information

The Supporting Information is available free of charge at https://pubs.acs.org/doi/10.1021/acsphotonics.2c00538.

Details of device design and characterization, as well as the spectrum reconstruction (PDF)

AUTHOR INFORMATION

Corresponding Author

Lan Li − *Key Laboratory of 3D Micro/Nano Fabrication and Characterization of Zhejiang Province, School of Engineering, Westlake University, Hangzhou 310024, China; Institute of Advanced Technology, Westlake Institute for Advanced Study, Hangzhou 310024, China;* orcid.org/0000-0002-9097-9157; Email: lilan@westlake.edu.cn

Authors

Chunlei Sun − *Key Laboratory of 3D Micro/Nano Fabrication and Characterization of Zhejiang Province, School of Engineering, Westlake University, Hangzhou 310024, China; Institute of Advanced Technology, Westlake Institute for Advanced Study, Hangzhou 310024, China*

Zequn Chen − *Key Laboratory of 3D Micro/Nano Fabrication and Characterization of Zhejiang Province, School of Engineering, Westlake University, Hangzhou 310024, China; Institute of Advanced Technology, Westlake Institute for Advanced Study, Hangzhou 310024, China*

Yuexin Yin − *Key Laboratory of 3D Micro/Nano Fabrication and Characterization of Zhejiang Province, School of Engineering, Westlake University, Hangzhou 310024, China; Institute of Advanced Technology, Westlake Institute for Advanced Study, Hangzhou 310024, China; State Key Laboratory of Integrated Optoelectronics, College of Electronic Science and Engineering, Jilin University, Changchun 130012, China*

Yuting Ye − *Key Laboratory of 3D Micro/Nano Fabrication and Characterization of Zhejiang Province, School of Engineering, Westlake University, Hangzhou 310024, China; Institute of Advanced Technology, Westlake Institute for Advanced Study, Hangzhou 310024, China*

Ye Luo − *Key Laboratory of 3D Micro/Nano Fabrication and Characterization of Zhejiang Province, School of Engineering, Westlake University, Hangzhou 310024, China; Institute of Advanced Technology, Westlake Institute for Advanced Study, Hangzhou 310024, China*

Hui Ma − *State Key Laboratory of Modern Optical Instrumentation, College of Information Science and Electronic Engineering, Zhejiang University, Hangzhou 310027, China*

Jialing Jian − *Key Laboratory of 3D Micro/Nano Fabrication and Characterization of Zhejiang Province, School of Engineering, Westlake University, Hangzhou 310024, China; Institute of Advanced Technology, Westlake Institute for Advanced Study, Hangzhou 310024, China*

Yilin Shi − *Key Laboratory of 3D Micro/Nano Fabrication and Characterization of Zhejiang Province, School of Engineering, Westlake University, Hangzhou 310024, China; Institute of Advanced Technology, Westlake Institute for Advanced Study, Hangzhou 310024, China*

Chuyu Zhong − *State Key Laboratory of Modern Optical Instrumentation, College of Information Science and Electronic Engineering, Zhejiang University, Hangzhou 310027, China*

Daming Zhang − *State Key Laboratory of Integrated Optoelectronics, College of Electronic Science and Engineering, Jilin University, Changchun 130012, China*

Hongtao Lin − *State Key Laboratory of Modern Optical Instrumentation, College of Information Science and Electronic Engineering, Zhejiang University, Hangzhou 310027, China;* orcid.org/0000-0001-7432-3644

Complete contact information is available at: https://pubs.acs.org/10.1021/acsphotonics.2c00538

Author Contributions

C.L.S. conceived the idea. Z.Q.C, Y.T.Y, H.M., and C.Y.Z. fabricated the devices. C.L.S., Y.X.Y, J.L.J., and Y.L.S. designed and carried out the experiments and performed data analysis. C.L.S., D.M.Z., H.T.L., and L.L. discussed the results. H.T.L. and L.L. supervised the project. All authors reviewed the manuscript.

Notes

The authors declare no competing financial interest.

https://doi.org/10.1021/acsphotonics.2c00538
ACS Photonics XXXX, XXX, XXX−XXX

■ ACKNOWLEDGMENTS

The authors acknowledge the financial support from National Key Research and Development Program of China (2019YFB2203003), National Natural Science Foundation of China (62175202, 12104375, and 91950204), Leading Innovative and Entrepreneur Team Introduction Program of Zhejiang (2020R01005), and Zhejiang Provincial Natural Science Foundation of China (LD22F040002). The authors also thank Westlake Center for Micro/Nano Fabrication and Instrumentation, Service Center for Physical Sciences and Molecular Sciences at Westlake University, and ZJU Micro-Nano Fabrication Center at Zhejiang University for the facility support.

■ REFERENCES

(1) Yang, Z.; Albrow-Owen, T.; Cai, W.; Hasan, T. Miniaturization of optical spectrometers. *Science* **2021**, *371*, No. eabe0722.
(2) Zhang, Z.; Wang, Y.; Tsang, H. K. Tandem Configuration of Microrings and Arrayed Waveguide Gratings for a High-Resolution and Broadband Stationary Optical Spectrometer at 860 nm. *ACS Photonics* **2021**, *8*, 1251−1257.
(3) Alshamrani, N.; Grieco, A.; Hong, B.; Fainman, Y. Miniaturized integrated spectrometer using a silicon ring-grating design. *Opt. Express* **2021**, *29*, 15279−15287.
(4) Calafiore, G.; Koshelev, A.; Dhuey, S.; Goltsov, A.; Sasorov, P.; Babin, S.; Yankov, V.; Cabrini, S.; Peroz, C. Holographic planar lightwave circuit for on-chip spectroscopy. *Light: Sci. Appl.* **2014**, *3*, No. e203.
(5) Zheng, S.; Cai, H.; Song, J.; Zou, J.; Liu, P. Y.; Lin, Z.; Kwong, D.-L.; Liu, A.-Q. A Single-Chip Integrated Spectrometer via Tunable Microring Resonator Array. *IEEE Photonics J.* **2019**, *11*, 1−9.
(6) Xia, Z.; Eftekhar, A. A.; Soltani, M.; Momeni, B.; Li, Q.; Chamanzar, M.; Yegnanarayanan, S.; Adibi, A. High resolution on-chip spectroscopy based on miniaturized microdonut resonators. *Opt. Express* **2011**, *19*, 12356−12364.
(7) Kyotoku, B. B. C.; Chen, L.; Lipson, M. Sub-nm resolution cavity enhanced micro-spectrometer. *Opt. Express* **2010**, *18*, 102−107.
(8) Zhang, L.; Chen, J.; Ma, C.; Li, W.; Qi, Z.; Xue, N. Research Progress on On-Chip Fourier Transform Spectrometer. *Laser Photonics Rev.* **2021**, *15*, 2100016.
(9) González-Andrade, D.; Dinh, T. T. D.; Guerber, S.; Vulliet, N.; Cremer, S.; Monfray, S.; Cassan, E.; Marris-Morini, D.; Boeuf, F.; Cheben, P.; Vivien, L.; Velasco, A. V.; Alonso-Ramos, C. Broadband Fourier-transform silicon nitride spectrometer with wide-area multi-aperture input. *Opt. Lett.* **2021**, *46*, 4021−4024.
(10) Velasco, A. V.; Cheben, P.; Bock, P. J.; Delâge, A.; Schmid, J. H.; Lapointe, J.; Janz, S.; Calvo, M. L.; Xu, D.-X.; Florjańczyk, M.; Vachon, M. High-resolution Fourier-transform spectrometer chip with microphotonic silicon spiral waveguides. *Opt. Lett.* **2013**, *38*, 706−708.
(11) Dinh, T. T. D.; González-Andrade, D.; Montesinos-Ballester, M.; Deniel, L.; Szelag, B.; Le Roux, X.; Cassan, E.; Marris-Morini, D.; Vivien, L.; Cheben, P.; Velasco, A. V.; Alonso-Ramos, C. Silicon photonic on-chip spatial heterodyne Fourier transform spectrometer exploiting the Jacquinot's advantage. *Opt. Lett.* **2021**, *46*, 1341−1344.
(12) Pohl, D.; Reig Escalé, M.; Madi, M.; Kaufmann, F.; Brotzer, P.; Sergeyev, A.; Guldimann, B.; Giaccari, P.; Alberti, E.; Meier, U.; Grange, R. An integrated broadband spectrometer on thin-film lithium niobate. *Nat. Photonics* **2020**, *14*, 24−29.
(13) Souza, M. C.; Grieco, A.; Frateschi, N. C.; Fainman, Y. Fourier transform spectrometer on silicon with thermo-optic non-linearity and dispersion correction. *Nat. Commun.* **2018**, *9*, 665.
(14) Li, A.; Davis, J.; Grieco, A.; Alshamrani, N.; Fainman, Y. Fabrication-tolerant Fourier transform spectrometer on silicon with broad bandwidth and high resolution. *Photonics Res.* **2020**, *8*, 219−224.
(15) Zheng, S. N.; Zou, J.; Cai, H.; Song, J. F.; Chin, L. K.; Liu, P. Y.; Lin, Z. P.; Kwong, D. L.; Liu, A. Q. Microring resonator-assisted Fourier transform spectrometer with enhanced resolution and large bandwidth in single chip solution. *Nat. Commun.* **2019**, *10*, 2349.
(16) Kita, D. M.; Miranda, B.; Favela, D.; Bono, D.; Michon, J.; Lin, H.; Gu, T.; Hu, J. High-performance and scalable on-chip digital Fourier transform spectroscopy. *Nat. Commun.* **2018**, *9*, 4405.
(17) Redding, B.; Liew, S. F.; Sarma, R.; Cao, H. Compact spectrometer based on a disordered photonic chip. *Nat. Photonics* **2013**, *7*, 746−751.
(18) Redding, B.; Fatt Liew, S.; Bromberg, Y.; Sarma, R.; Cao, H. Evanescently coupled multimode spiral spectrometer. *Optica* **2016**, *3*, 956−962.
(19) Zhang, Z.; Li, Y.; Wang, Y.; Yu, Z.; Sun, X.; Tsang, H. K. Compact High Resolution Speckle Spectrometer by Using Linear Coherent Integrated Network on Silicon Nitride Platform at 776 nm. *Laser Photonics Rev.* **2021**, *15*, 2100039.
(20) Hadibrata, W.; Noh, H.; Wei, H.; Krishnaswamy, S.; Aydin, K. Compact, High-resolution Inverse-Designed On-Chip Spectrometer Based on Tailored Disorder Modes. *Laser Photonics Rev.* **2021**, *15*, 2000556.
(21) Li, A.; Fainman, Y. On-chip spectrometers using stratified waveguide filters. *Nat. Commun.* **2021**, *12*, 2704.
(22) Sun, C.; Yin, Y.; Chen, Z.; Ye, Y.; Luo, Y.; Ma, H.; Wang, L.; Wei, M.; Jian, J.; Tang, R.; Dai, H.; Wu, J.; Li, J.; Zhang, D.; Lin, H.; Li, L. Tunable narrow-band single-channel add-drop integrated optical filter with ultrawide FSR. *PhotoniX* **2022**, *3*, 1−12.
(23) Li, A.; Fainman, Y. Integrated Silicon Fourier Transform Spectrometer with Broad Bandwidth and Ultra-High Resolution. *Laser Photonics Rev.* **2021**, *15*, 2000358.
(24) Nauriyal, J.; Song, M.; Yu, R.; Cardenas, J. Fiber-to-chip fusion splicing for low-loss photonic packaging. *Optica* **2019**, *6*, 549−552.
(25) Zhang, W.; Ebert, M.; Reynolds, J.; Chen, B.; Yan, X.; Du, H.; Banakar, M.; Tran, D.; Littlejohns, C.; Reed, G.; Thomson, D. J. Buried 3D spot-size converters for silicon photonics. *Optica* **2021**, *8*, 1102−1108.
(26) Gehring, H.; Blaicher, M.; Hartmann, W.; Varytis, P.; Busch, K.; Wegener, M.; Pernice, W. Low-loss fiber-to-chip couplers with ultrawide optical bandwidth. *APL Photonics* **2019**, *4*, 010801.

https://doi.org/10.1021/acsphotonics.2c00538
ACS Photonics XXXX, XXX, XXX−XXX